Experimental absolute electron impact ionization cross-sections of Cl_2

2004 New J. Phys. 6 118

(http://iopscience.iop.org/1367-2630/6/1/118)

New Journal of Physics
An Institute of Physics and Deutsche Physikalische Gesellschaft Journal

Experimental absolute electron impact ionization cross-sections of Cl_2

R Basner[1] **and K Becker**[2]

[1] Institut für Niedertemperatur-Plasmaphysik, Friedrich-Ludwig-Jahn-Strasse 19, D-17489 Greifswald, Germany
[2] Department of Physics and Engineering Physics and Center for Environmental Systems, Stevens Institute of Technology, Hoboken, NJ 07030, USA
E-mail: basner@inp-greifswald.de and kbecker@stevens.edu

New Journal of Physics **6** (2004) 118
Received 1 April 2004
Published 17 September 2004
Online at http://www.njp.org/
doi:10.1088/1367-2630/6/1/118

Abstract. We measured absolute partial cross-sections for the formation of Cl_2^+, Cl_2^{2+}, Cl^+ and Cl^{2+} ions following electron impact on molecular chlorine (Cl_2) from threshold to 900 eV using a time-of-flight mass spectrometer. The ion spectrum at all impact energies is dominated by the singly charged ions with maximum cross-section values of 4.6×10^{-16} cm^2 for Cl_2^+ at 32 eV and 4.0×10^{-16} cm^2 for Cl^+ at 70 eV. The cross-sections for the formation of the doubly charged ions are more than one order of magnitude lower. Double ionization processes account for about 6% of the total ion yield at 70 eV. The absolute total ionization cross-section of Cl_2 was obtained as the sum of all measured partial ionization cross-sections. To the extent possible, a comparison of our results with other available measured and calculated data is made.

Contents

PII: S1367-2630(04)78722-4

1. Introduction

In an effort to understand the electron ionization processes and develop models of the chemistry occurring in technologically important low-temperature plasmas, various reliable cross-sections for the electron impact ionization and dissociative ionization are needed. Recent work on the interactions of molecular chlorine (Cl_2) with electrons is largely motivated by the importance of this molecule for plasma-etching applications. Cl_2 is widely used as the main constituent or an admixture in processing plasmas feed gas mixtures that are used to etch silicon [1]–[4], different other semiconductor materials [5]–[8] and various metals and metal oxides [9]–[12].

Recently, Christophorou and Olthoff [13] published a comprehensive review of critically evaluated and assessed data for fundamental interactions of low-energy electrons with Cl_2 by updating and expanding previous data compilations [14]. Although the electron impact and ion transport database of Cl_2 is more extensive compared with similar databases for other plasma processing gases, it is not complete and a significant number of the available data have not been confirmed by more than one independent measurement or by a stringent comparison between measurement and calculation [13]. Total electron impact ionization cross-sections of Cl_2 were measured by Center and Mandl [15], Kurepa and Belic [16], Stevie and Vasile [17] and Srivastava and Boivin in [13]. The four data sets differ in the magnitude of the reported cross-sections as well as in the measured energy dependence. The cross-section values vary from 0.25×10^{-16} to 5.1×10^{-16} cm^2 at 20 eV impact energy and from 5.5×10^{-16} to 7.1×10^{-16} cm^2 at 70 eV [13]. The results of recent calculations of the total Cl_2 ionization cross-section were also summarized in the review of Christophorou and Olthoff [13]. These calculations show noticeable differences between each other, but are in reasonable agreement (within the margin of experimental uncertainty) with the measurements of Stevie and Vasile [17]. The database on partial ionization cross-sections for Cl_2 is rather limited. Calandra *et al* [18] measured relative partial cross-sections for the formation of Cl_2^+, Cl^+ and Cl^{2+} in the energy range from 25 to 200 eV using a time-of-light mass spectrometer (TOF-MS). Recently, Pal *et al* [19] have calculated absolute partial cross-sections for the formation of Cl_2^+, Cl_2^{2+} and Cl^+ based on the measured and normalized photo-ionization cross-sections of Samson and Angel [20]. However, the measured branching ratio Cl^+/Cl_2^+ [18] is much larger (about four times at an impact energy of 35 eV) than the ratio of the calculated cross-sections [19]. Also, the measured and calculated energy dependences are completely different, even if the contributions of Cl^+ ions from multiple ionization are removed from the measured data. Obviously, the availability of reliable absolute ionization data for Cl_2 is unsatisfactory.

Here, we report measured electron-impact ionization cross-section data for Cl_2 in the energy range from threshold to 900 eV obtained in a TOF-MS that allows us to determine reliable absolute partial ionization cross-sections without mass discrimination of the energetic fragment ions.

2. Experimental details

The measurements were carried out using a TOF-MS shown schematically in figure 1. The instrument and the data acquisition and analysis procedures have been described in detail before [21]–[23] and the reliability of this mass spectrometric technique for the measurement for absolute partial ionization cross-sections of energetic fragment ions was demonstrated for the plasma processing gases $TiCl_4$, SiF_4, CF_4/C_2F_6, B_2H_6 and WF_6 [21]–[25]. Briefly, the TOF-MS

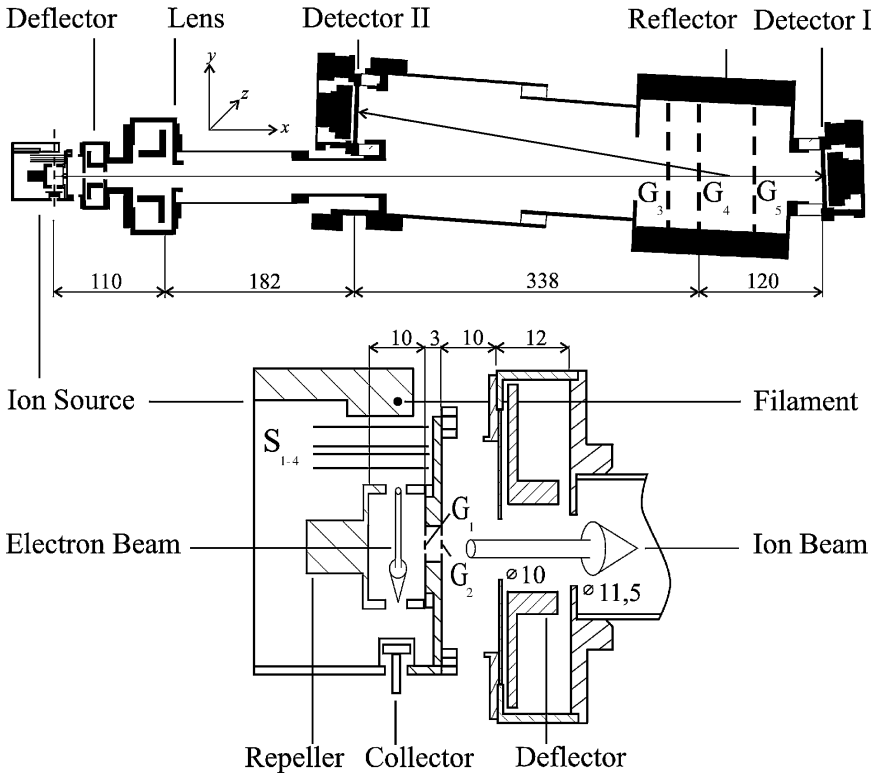

Figure 1. Schematic diagram of the TOF-MS and a detailed view of the electron impact ion source used in the present study (all dimensions are in mm).

can be operated either in a linear mode using detector I or in a reflection mode using the reflector (grids: G_3–G_5) and detector II. In the present study, all measurements for the determination of the partial ionization cross-sections were performed with the TOF-MS operated in the linear mode to ensure complete transport of energetic fragment ions from the ion source to the detector and to reduce the data collection time by operating the instrument at a maximum repetition frequency of 20 kHz. Additionally, the reflection mode was used successfully to confirm the results at fixed impact energy of 70 eV. The ion source chamber was filled with a well-defined Cl_2/Ar mixture through precision leak valves up to partial pressures of about 1×10^{-4} Pa in an effort to facilitate the simultaneous measurements of the ions from Cl_2 and Ar under identical operating conditions. The relative partial Cl_2 ionization cross-sections were put on an absolute scale by normalization relative to the partial Ar^+ ionization cross-section of 2.52×10^{-16} cm^2 at 70 eV [26]. Taking into account the uncertainties of ±5% in the Ar reference cross-section [26], the statistical uncertainty in our pressure measurement of ±3% and an uncertainty of typically ±3–7% resulting from the counting statistics, we assign an overall uncertainty of ±15% to the absolute ionization cross-sections reported here.

Typically, the electron gun was operated using electron pulses of 100 ns width. The electron beam has a diameter of about 0.6 mm in the interaction region and the amplitude of the electron pulse was in the range from 1 to 10 μA with an energy spread of about 0.5 eV (FWHM). The impact energy was varied from 5 to 900 eV and the electron beam was guided by a weak magnetic field (200 G). A voltage of 1 kV (extraction fields of 1 kV cm^{-1}) was applied to the repeller, roughly 10 ns after the incident electron pulse passed through the ionization region.

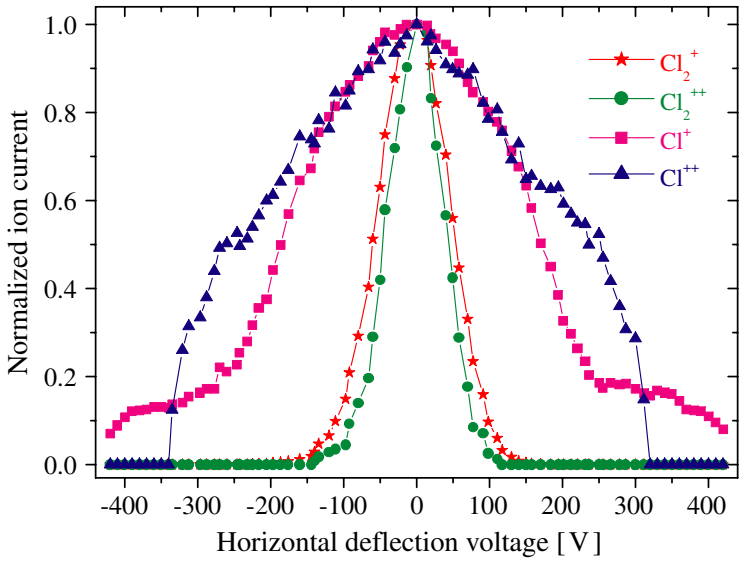

Figure 2. Normalized ion beam currents of Cl_2^+, Cl^+, Cl_2^{2+} and Cl^{2+} as a function of the horizontal deflection voltage at 70 eV impact energy. These data were obtained with a double-focusing sector field mass spectrometer.

This extraction pulse accelerates the ions formed by electron impact towards the grounded ion source exit aperture and the entrance electrode of the flight tube, which is held at a −2.8 kV bias voltage. We maintained operating conditions under which 100% ion transmission of all ions from the ion source to the detector was established with the exception of ion losses at the grids G_1 and G_2. The output signal from the respective MCP passes a preamplifier, a constant fraction discriminator and is recorded with a 2 GHz multiscaler (Model 7886; FAST ComTec) with a time resolution of 500 ps. Our TOF-MS was operated in such a way that no more than one ion of the most intense ion signal was created during each electron pulse. This resulted in low overall count rates and comparatively long data acquisition times, but ensured, on the other hand, that dead time corrections to the recorded signal rates were negligible.

3. Results and discussions

The mass spectra of positive ions resulting from electron impact on Cl_2 at 70 eV impact energy derived from measurements carried out with the TOF-MS operated in the linear mode and in the reflection mode confirm the expected isotopic distributions due to the natural isotopic abundances of 75.8% for ^{35}Cl and 24.2% for ^{37}Cl [27]. We observe a relative intensity of Cl^+ that is 10% higher compared with the mass spectrum found in the NIST database [28]. The reason for this discrepancy may be the optimized detection efficiency of our TOF-MS for energetic fragment ions. This optimization is usually not done for quadrupole mass spectrometers that are most commonly used in analytical mass spectrometry. We carried out qualitative checks of the excess kinetic energy for fragment ions Cl^+ and Cl^{2+} by performing a full horizontal sweep of the extracted ion beam using a double-focusing mass spectrometer and comparing the shapes with the Cl_2^+ and Cl_2^{2+} ion signals, which are characteristic of a beam of ions without excess kinetic energy and show identical shapes as Ar^+ and Ar^{2+} [21, 24]. The curves of the two fragment ions (see figure 2) show a distinct broadening which is indicative of a broad distribution of excess

kinetic energies. The Cl_2 mass spectrum in the NIST database [28] does not show any doubly charged ion signal at all. We identified the Cl^{2+} ion at mass numbers 17.5 and 18.5 and in addition the $^{35}Cl^{37}Cl^{2+}$ ion at mass number 36. Using the known isotopic abundances, we calculated the respective $^{35}Cl_2{}^{2+}$ and $^{37}Cl_2{}^{2+}$ ion currents and corrected the $^{35}Cl^{+}$ and $^{37}Cl^{+}$ ion signals at the same mass numbers for all impact energies. The partial ionization cross-sections were then obtained by adding the individual isotope contributions. The thresholds of the particular ionization curves with their respective uncertainties confirm the known values of the appearance energies for $Cl_2{}^{+}$, $Cl_2{}^{2+}$, Cl^{+} [13, 29] and Cl^{2+} [18].

The numerical values of the partial ionization cross-sections for the formation of singly charged ions, the partial counting ionization cross-sections for the formation of doubly charged ions, and the total ionization cross-section (the charge-weighted sum of all partial cross-sections) as a function of the energy of the ionizing electrons from threshold to 900 eV are given in table 1. The corresponding cross-section curves of the singly and doubly charged ions are shown in figure 3(a) (singly charged ions) and figure 3(b) (doubly charged ions) from threshold to 200 eV. It is obvious from the cross-section curves shown in figures 3(a) and (b) that direct ionization of Cl_2 to form $Cl_2{}^{+}$ is the dominant process in the entire range of impact energies, although above 40 eV almost as many Cl^{+} ions are formed as $Cl_2{}^{+}$ ions. The cross-sections of $Cl_2{}^{+}$ increase rapidly from threshold to a narrow maximum of 4.59×10^{-16} cm at 32 eV and then decrease to a minimum at 46 eV and increase again to a broad maximum of 4.55×10^{-16} cm^2 at 80 eV followed by a gradual decrease towards higher impact energy. This energy dependence of the cross-sections, which was also found for the electron impact ionization of $TiCl_4$ [21], may be a result of an auto-ionization channel competing with direct ionization [30]. This indirect ionization process is expected to be more prominent in the low-energy range and is a resonance process. The cross-section curves of the other three ions all show the more conventional cross-section shape, which shows an increase from threshold to a maximum around 70–100 eV followed by a gradual decrease towards higher impact energies. Figure 3(a) also shows the calculated partial cross-sections of Pal *et al* [19] for $Cl_2{}^{+}$ and Cl^{+}. Their results differ from our data for $Cl_2{}^{+}$ in the energy dependence and in the absolute values and for Cl^{+} in the absolute values by a factor of 4.

The ion spectrum in the lower energy region, which is of special interest for low-temperature plasma technology, is dominated by $Cl_2{}^{+}$. For example, $Cl_2{}^{+}$ accounts for 95% of the total ionization cross-section value at 15 eV and for 88% at 20 eV.

Doubly charged ions appear at energies above 32 eV in case of $Cl_2{}^{2+}$ and above 40 eV for Cl^{2+}. These cross-sections reach their maximum values at energies of 80 and 100 eV, respectively (see table 1 and figure 3(b)). The maximum cross-section values are more than one order of magnitude lower compared with those of the singly charged ions. The charge-weighted sum of the doubly charged fragment ions accounts for about 7.6% of the total ionization cross-section of Cl_2 at 100 eV. Figure 3(b) also shows the calculated partial cross-sections of Pal *et al* [19] for $Cl_2{}^{2+}$. Their result for $Cl_2{}^{2+}$ differs from ours in the energy dependence and in the absolute value by a factor of 24.

It is possible to compare the energy dependence of the partial cross-sections measured as part of this work with the relative partial cross-sections reported recently by Calandra *et al* [18] in the energy range from 25 to 200 eV. Since their measurements were not absolute, we can only compare the ratio of partial cross-sections. Figure 4 shows the ratios of the partial cross-sections $Q_r(Cl^{+}/Cl_2{}^{+})$ and $Q_r(Cl^{2+}/Cl_2{}^{+})$ from our data in comparison with the data of [18]. Since Calandra *et al* [18] did not report separate cross-section curves for the formation of Cl^{+} and $Cl_2{}^{2+}$,

Table 1. Absolute partial counting and total (charge-weighted) electron impact ionization cross-sections for Cl_2 as a function of electron energy.

Electron energy (eV)	Ionization cross-section (10^{-16} cm^2)				
	Cl_2^+	Cl^+	Cl_2^{2+}	Cl^{2+}	Total
12	0.100				0.100
13	0.346	0.014			0.360
14	0.746	0.032			0.778
15	1.13	0.055			1.19
16	1.58	0.081			1.66
17	2.00	0.126			2.13
18	2.39	0.209			2.60
19	2.72	0.297			3.02
20	3.13	0.435			3.57
22	3.65	0.715			4.37
24	4.00	1.08			5.08
26	4.30	1.43			5.73
28	4.49	1.85			6.34
30	4.57	2.18			6.75
32	4.59	2.67			7.26
34	4.54	2.93			7.47
36	4.44	3.13	0.003		7.58
38	4.36	3.30	0.010		7.68
40	4.31	3.40	0.021		7.75
42	4.28	3.55	0.030		7.89
44	4.26	3.63	0.048	0.005	7.99
46	4.25	3.68	0.070	0.013	8.10
48	4.27	3.74	0.089	0.033	8.26
50	4.31	3.80	0.099	0.045	8.40
52.5	4.34	3.85	0.104	0.078	8.56
55	4.38	3.87	0.109	0.099	8.67
57.5	4.41	3.90	0.112	0.112	8.76
60	4.43	3.95	0.117	0.121	8.86
65	4.49	3.99	0.123	0.139	9.00
70	4.52	4.03	0.127	0.152	9.11
80	4.55	4.01	0.129	0.190	9.20
90	4.51	3.9	0.128	0.207	9.08
100	4.50	3.84	0.123	0.221	9.03
120	4.41	3.67	0.106	0.216	8.73
140	4.17	3.35	0.096	0.205	8.12
160	4.12	3.23	0.084	0.187	7.89
180	4.03	3.04	0.075	0.171	7.56
200	3.87	2.86	0.068	0.158	7.18
300	3.22	2.16	0.054	0.122	5.73
400	2.79	1.76	0.043	0.102	4.84
500	2.45	1.45	0.029	0.091	4.14
600	2.14	1.25	0.020	0.078	3.59
700	1.98	1.11	0.016	0.071	3.26
800	1.80	0.973	0.012	0.063	2.92
900	1.63	0.890	0.011	0.062	2.67

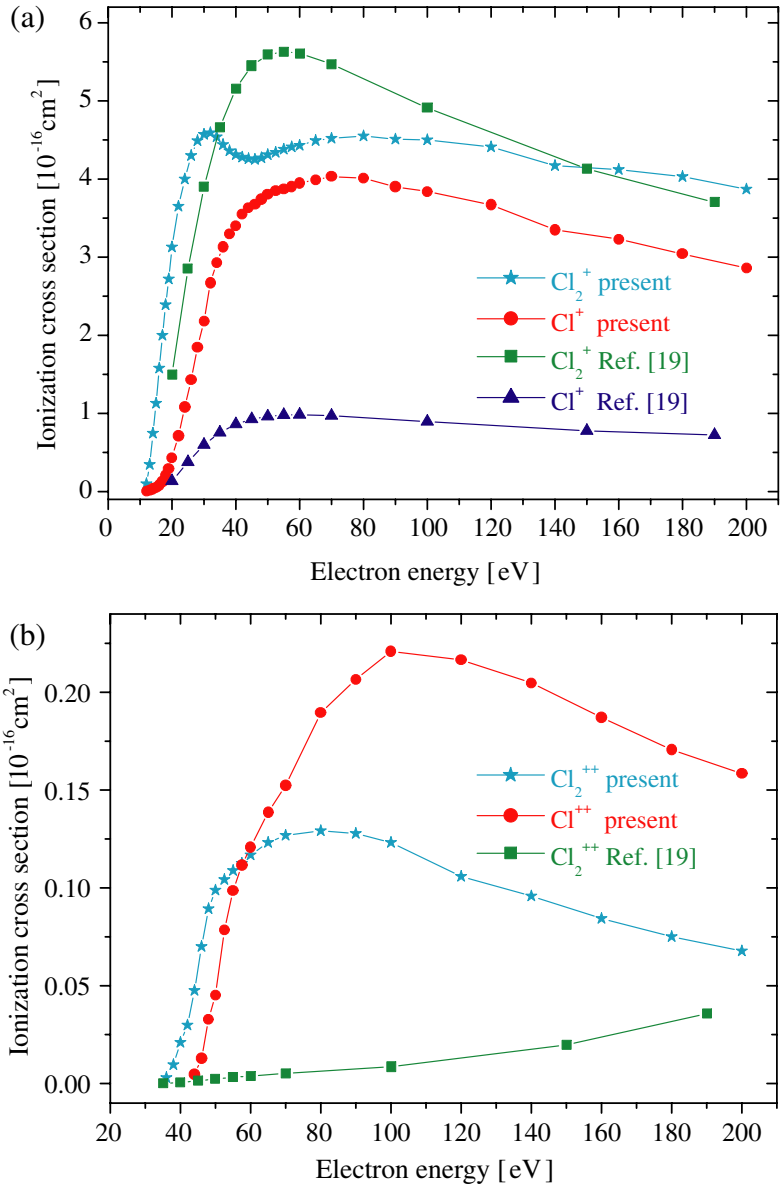

Figure 3. (a) Present absolute partial Cl_2 ionization cross-sections of Cl_2^+ and Cl^+ along with calculated data from [19] as a function of electron energy up to 200 eV. (b) Present absolute partial Cl_2 ionization cross-sections of Cl_2^{2+} and Cl^{2+} along with calculated data from [19] as a function of electron energy up to 200 eV.

we also included the cross-section ratio $Q_r((Cl^+ + Cl_2^{2+})/Cl_2^+)$ based on our data. Within the margin of error there is good agreement between the cross-section ratios derived from our data and the data of [18].

The present total Cl_2 ionization cross-section is shown in figure 5 up to 200 eV along with the present total single Cl_2 ionization cross-section and some previously reported experimental and theoretical results. The total ionization cross-section curve of molecular chlorine (last column of table 1) is derived as the charge-weighted sum of the four partial ionization cross-sections reported here. The total ionization cross-section exhibits a maximum at 80 eV with a peak value

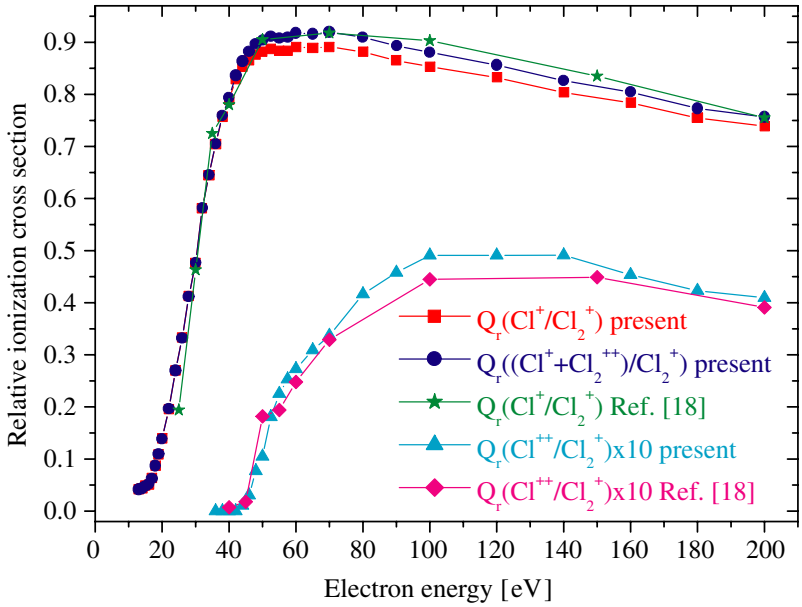

Figure 4. Present cross-section ratios $Q_r(Cl^+/Cl_2^+)$, $Q_r((Cl^+ + Cl_2^{2+})/Cl_2^+)$, and $Q_r(Cl^{2+}/Cl_2^+) \times 10$ along with measured data from [18] as a function of electron energy up to 200 eV.

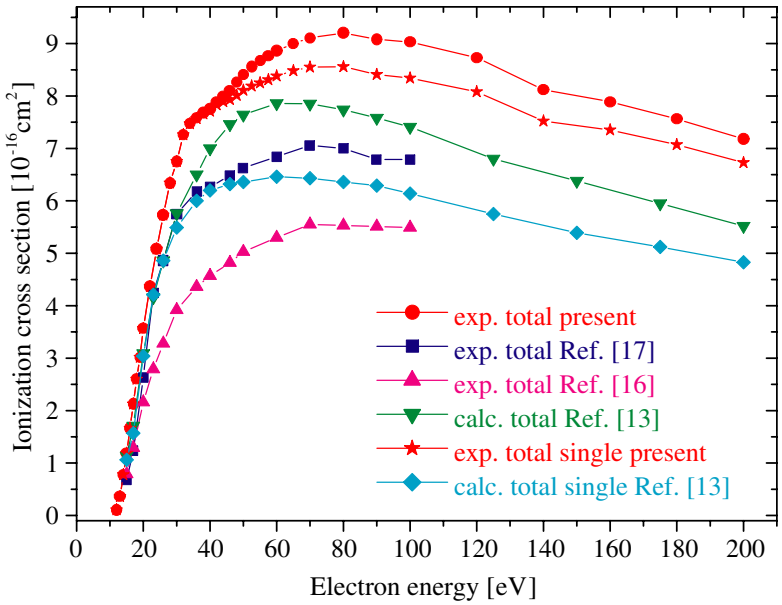

Figure 5. Present absolute total Cl_2 ionization cross-sections and absolute total single Cl_2 ionization cross-sections along with previously reported experimental (exp.) and theoretical (calc.) results as a function of electron energy up to 200 eV.

of 9.2×10^{-16} cm^2. Also shown in figure 5 are the total cross-sections from Kurepa and Belic [16], Stevie and Vasile [17], and an unpublished calculation taken from [13]. Additionally shown in figure 5 are unpublished calculations for the total single ionization cross-section also taken from [13]. Clearly, our results exceed all the other data with increasing impact energy including

the suggested total cross-section of Christophorou and Olthoff [13], which is an average of data from [16, 17]. We note that several independent measurements with the TOF-MS in the reflection mode confirmed the absolute cross-section values reported here at the fixed impact energy of 70 eV.

4. Conclusions

We measured for the first time the absolute partial electron ionization cross-sections for the Cl_2 molecule using a time-of-flight mass spectrometric technique. A complete set of the absolute ionization cross-sections for the formation of Cl_2^+, Cl_2^{2+}, Cl^+ and Cl^{2+} from Cl_2 was determined in the energy range from threshold to 900 eV. Direct ionization of Cl_2 to form Cl_2^+ was found to be the dominant process in the entire range of impact energies and shows a pronounced maximum around 30 eV. The energy dependence and the relative partial ionization cross-section are in excellent agreement with recently measured relative cross-sections [18], but show significant discrepancies in comparison with theoretical predictions [19]. The derived absolute total ionization cross-section values are generally higher than all previous experimental and calculated data sets. The absolute cross-section values measured here are an essential contribution to complete the database on electron interactions with molecular chlorine, which is indispensable for a microscopic understanding and the detailed modelling of Cl_2-containing plasmas. The data presented here are also important for the critical evaluation of quantitative mass spectrometric plasma diagnostics data.

Acknowledgments

KB acknowledges financial support for this work from the US Department of Energy, Office of Science.

References

[1] Bloor D, Brook R J, Flemings M C, Mahajahn S and Cahn R W 1993 *Ion Etching and Plasma Etching of Silicon* (New York: Pergamon)
[2] Kiehlbauch M W and Graves D B 2003 *J. Vac. Sci. Technol.* A **21** 116
[3] Bogart K H A and Donnelly V M 2000 *J. Appl. Phys.* **87** 8351
[4] Ullal S J, Kim T W, Vahedi V and Aydil E S 2003 *J. Vac. Sci. Technol.* A **21** 589
[5] Shul R J and Pearton S J 2000 *Handbook of Advanced Plasma Processing Techniques* (Berlin: Springer) p 469
[6] Hahn Y B, Hays D C, Cho H, Jung K B, Abernathy C R, Pearton S J and Shul R J 1999 *Appl. Surf. Sci.* **147** 207
[7] Hahn Y B, Hays D C, Cho H, Jung K B, Abernathy C R, Pearton S J and Shul R J 1999 *Appl. Surf. Sci.* **147** 215
[8] Zhu K, Kuryatkov V, Borisov B, Kipshidze G, Nikishin S A, Temkin H and Holtz M 2002 *Appl. Phys. Lett.* **81** 4688
[9] Tachi S 2003 *J. Vac. Sci. Technol.* A **21** 131
[10] Malyshev M V, Donelly V M, Downey S W, Colonell J I and Layadi N 2000 *J. Vac. Sci. Technol.* A **18** 849
[11] Lim W T, Baek I K, Lee J W, Lee E S, Jeon M H, Cho G S, Heo Y W, Norton D P and Pearton S J 2003 *Appl. Phys. Lett.* **83** 3105
[12] Pelhos K, Donelly V M, Kornblit A, Green M L, Van Dover R B, Manchanda L, Hu Y, Morris M and Bower E 2001 *J. Vac. Sci. Technol.* A **219** 1361

[13] Christophorou L G and Olthoff J K 2004 *Fundamental Electron Interactions with Plasma Processing Gases* (New York: Kluwer Academic/Plenum) p 449
[14] Christophorou L G and Olthoff J K 1999 *J. Phys. Chem. Ref. Data* **28** 131
[15] Center R E and Mandl A 1972 *J. Chem. Phys.* **57** 4104
[16] Kurepa M V and Belic D S 1978 *J. Phys. B: At. Mol. Phys.* **11** 3719
[17] Stevie F A and Vasile M J 1981 *J. Chem. Phys.* **74** 5106
[18] Calandra P, O'Connor C S S and Price S D 2000 *J. Chem. Phys.* **112** 10821
[19] Pal S, Bhatt P and Kumar J 2003 *Int. J. Mass Spectrom.* **229** 151
[20] Samson J A R and Angel G C 1987 *J. Chem. Phys.* **86** 1814
[21] Basner R, Schmidt M, Becker K, Tarnovsky V and Deutsch H 2000 *Thin Solid Films* **374** 291
[22] Basner R, Schmidt M, Denisov E, Becker K and Deutsch H 2001 *J. Chem. Phys.* **114** 1170
[23] Basner R, Schmidt M, Denisov E, Lopata P, Becker K and Deutsch H 2002 *Int. J. Mass Spectrom.* **214** 365
[24] Basner R, Schmidt M and Becker K 2003 *J. Chem. Phys.* **118** 2153
[25] Basner R, Schmidt M and Becker K 2004 *Int. J. Mass Spectrom.* **233** 25
[26] Rejoub R, Lindsay B G and Stebbings R F 2002 *Phys. Rev.* A **65** 042713-1
[27] Lide D R 2002 *CRC Handbook of Chemistry and Physics 2001–2002* (Boca Raton, FL: CRC Press) pp 11–57
[28] NIST Database (webbook.nist.gov/chemistry/form-ser.html)
[29] Rosenstock H M, Draxl K, Steiner B W and Herron J T 1977 *J. Phys. Chem. Ref. Data* **6** I-453
[30] Märk T D and Dunn G H 1985 *Electron Impact Ionization* (Vienna: Springer) p 140